INFLUENCE OF ELASTIC PROPERTIES DEPENDENCE OF THE STRESS STATE ON BUCKLING CONDITIONS IN COMPOSITE STRUCTURES

Alexey N. Fedorenko [1], Boris N. Fedulov [1] and Evgeny V. Lomakin [1,2]

[1]Moscow Aviation Institute, Aircraft Design Center, Volokolamskoe Road 4 Moscow, Russia
Email: alexey.n.fedorenko@gmail.com, Web Page: http://www.mai.ru
[2]Lomonosov Moscow State University, Faculty of Mechanics and Mathematics, GSP-1, 1 Leninskiye Gory, Main Building, Moscow, Russia
Email: evlomakin@yandex.ru, Web Page: http://www.msu.ru

Keywords: composite laminate, nonlinear elasticity, thin-walled structure, buckling

Abstract
This paper demonstrates, as an illustration of the influence of stress state susceptibility of material properties on the behavior of composite structures, the solution of problem of buckling and postbuckling analysis of stiffened thin-walled composite cylinder, where straightforward approach with linear elastic theory leads to inaccurate results even on initial stage of loading. During buckling process, a stress state in material point is able to change significantly and it should be taken into account, for example, for materials with different elastic moduli in tension and compression and for other stress state types, too. Nonlinear elastic model based on the use of triaxiality parameter is considered and implemented in FEA software to capture effects related with sensitivity of material elastic properties to the stress state.

1. Introduction

Buckling problem is quite important for the engineering practice, mostly, in cases of lightweight structures. The use of composites makes possible to reduce the weight of the structure but adds problems in choice of reliable methods to model buckling and postbuckling behavior of structures, especially if they contain thin-walled components [1, 2] . One of the problem is the choice of correct elastic properties of composite material for the analysis. Elastic characteristics of composite material depend on the type of loading and the analysis of uniaxial tension/compression tests usually demonstrate an essential difference of them [3]. The buckling analysis usually assumes compression of the structure, and the choice of elastic constants obtained in compression tests leads to more accurate results, but does not guarantee a good correlation with experiments in case of postbuckling analysis due to ignoring of some regions with predominant tension stress state. Another important effect is the nonlinearity of stress-strain diagram under shear loading [4, 5]. A possible way of stress-state susceptibility consideration is the usage of material models that take into account stiffness variation depending on the types of loading. Further development of nonlinear elastic model in problems related to buckling and postbuckling analysis for the structures of composite materials up to failure is the introduction of material degradation model to take into account the material's properties reduction due to damage in conjuction with nonlinear elasticity [6, 7].
The model presented in this work is based on the usage of triaxiality parameter, which characterizes the stress state in a material [8, 9, 10]. The main goals of this study are to implement nonlinear elastic model to FEM software, test it on engineering problem of thin-walled composite structures compression and compare the results with conventional approach.

2. Anisotropic elastic model susceptible to stress state and nonlinear shear

Nonlinear elastic model is based on formulations described in [11]. Stress triaxiality parameter ξ is used to formalize stress state:

$\xi = \sigma/\sigma_0$,

where $\sigma = 1/3\sigma_{ii}$ is the hydrostatic stress component, $\sigma_0 = \sqrt{3/2 S_{ij}S_{ij}}$ - is von Mises equivalent stress, $S_{ij} = \sigma_{ij} - \sigma\delta_{ij}$ is stress deviator components.

For the development of nonlinear shear material model, the parameter that represents the degree of shear stresses or deformations is formulated in the following form:

$$Q = D_{ij}\sigma_{ij}, \tag{1}$$

where D_{ij} tensor have the following representation in coordinate system coincident with the orientation of anisotropy axes:

$$D_{ij} = \begin{bmatrix} 0 & 1/2 & 0 \\ 1/2 & 0 & 0 \\ 0 & 0 & 0 \end{bmatrix}. \tag{2}$$

Elastic potential can be represented in the form dependent on stress triaxiality and shear parameter as shown below:

$$\Phi = \frac{1}{2}A_{ijkl}(\xi, Q)\sigma_{ij}\sigma_{kl} \tag{3}$$

In case of plane stress conditions the value of the parameter ξ is limited $-3/2 \leq \xi \leq 3/2$ and the constitutive equations obtained on the base of potential Eq.3 can be represented in following form:

$$\varepsilon_{11} = A_{1111}(\xi)\sigma_{11} + A_{1122}(\xi)\sigma_{22} + \left[\left(\frac{1}{3\xi} + \frac{3}{2}\xi\right)\sigma - \frac{3}{2}\xi\sigma_{11}\right]\Phi_1\sigma_0^{-2},$$

$$\varepsilon_{22} = A_{1122}(\xi)\sigma_{11} + A_{2222}(\xi)\sigma_{22} + \left[\left(\frac{1}{3\xi} + \frac{3}{2}\xi\right)\sigma - \frac{3}{2}\xi\sigma_{22}\right]\Phi_1\sigma_0^{-2},$$

$$\varepsilon_{12} = \left[\left(A_{1212}(\xi, Q) + \frac{1}{2}\frac{\partial A_{1212}(\xi,Q)}{\partial Q}\right) - \frac{3}{2}\xi\Phi_1\sigma_0^{-2}\right]\sigma_{12}, \tag{4}$$

$$\Phi_1 = \frac{1}{2}[A'_{1111}(\xi)\sigma_{11}^2 + A'_{2222}(\xi)\sigma_{22}^2 + 2A'_{1122}(\xi)\sigma_{11}\sigma_{22} + A'_{1212}(\xi)\sigma_{12}^2],$$

where prime denotes the derivative with respect to parameter ξ and, according to Eq. 1 and Eq. 2, the dependency on parameter Q remains only in $A_{1212}(\xi, Q)$.

Using polynomial substitution $A_{1212}(\xi, Q) = \sum_n C_n(\xi) Q^n$ to expression for ε_{12} in Eq.4 and assuming $B_n(\xi) = (1 + n/2)C_n(\xi)$ one can obtain

$$\varepsilon_{12} = \left[B(\xi, Q) - \frac{3}{2}\xi\Phi_1\sigma_0^{-2}\right]\sigma_{12}, \tag{5}$$

where $B(\xi, Q)$ is an arbitrary function that can be approximated by polynomial dependency.

The determination of functional dependencies of coefficients A_{ijkl} is a complex problem and requires an extensive test data obtained under combined loading conditions. In practical way, the piecewise linear functions could be used, but following the idea to keep less number of parameters in the model one can define

$$A_{1111}(\xi) = a_{11}^0 + c_{11}\xi,$$

$$A_{2222}(\xi) = a_{22}^0 + c_{22}\xi, \tag{6}$$

$$A_{1122}(\xi) = a_{12}^0 + c_{12}\xi,$$

with constant a_{ij}^0 and c_{ij}.

Alexey N. Fedorenko, Boris N. Fedulov and Evgeny V. Lomakin

The coefficients A_{ijkl} in general case are not arbitrary. In particular, coefficients have to guarantee positive-definiteness of the potential Eq.3. Analytical solution for finding restrictions for coefficients in linear relations Eq.6 is still not obtained, but positive-definiteness of potential for predefined coefficients can be verified numerically for the range of ξ between -2/3 and +2/3 in the case of plane stress conditions.

In case of pure shear $\xi = 0$, and Eq.5 can be reduced to expression $\varepsilon_{12} = B(0, Q)\sigma_{12}$. Since $B(0, Q)$ assumes the polynomial form, it can be taken in the form proposed by Tsai and Hahn [4]:

$$\varepsilon_{12} = \frac{1}{2}\left[\frac{1}{G} + \alpha\sigma_{12}^2 - 3\xi\Phi_1\sigma_0^{-2}\right]\sigma_{12}, \tag{7}$$

where G is a constant shear modulus on initial stage of deformation that commonly used for linear elastic relations, and α is a coefficient which can be defined from shear loading diagram.

It should be noted, that Eq.7 assumes simplification of independence on stress triaxiality: $B(\xi, Q) = B(Q)$.

Now constitutive relations of Eq.4 with simplification for shear component are defined, and final problem is the choice of constants in Eq.6 for analyzed material.

3. Thin-walled composite cylinder test problem
3.1. Description of experiment

Experimental results of Bisagni's research [12] were used as an example of detailed test data with extensive measurements. This work contains experimental data obtained from buckling and post-buckling tests performed until the collapse of stiffened composite cylindrical shell. According to experimental data, the tested cylinder has internal diameter and an overall length of 700 mm, including two tabs provided at the top and at the bottom surfaces for fixing the shell into the test equipment. The cylinder is rigidly fixed through end tabs and loaded to compression applying displacement up to failure. The actual length is therefore limited within the central part of the cylinder height and is equal to 540 mm. The shell is reinforced by eight L-shaped stringers, equally oriented and equally spaced in circumferential direction. The blade of the stiffeners is 25 mm long, while the flange attached to the skin of the cylinder is 32 mm long. The cylinder dimensions presented in Table 1. The shell of carbon fiber reinforced plastics (CFRP) is made of fabric tape with material properties shown in Table 2, as given in [12].

Table 1. Stringer-reinforced cylinder characteristics

Parameter	Value
Shell diameter [mm]	700
Shell length [mm]	700
Stringers:	
Number	8
L length [mm]	700
L width [mm]	25×32
Lay-up:	
Skin	[+45°/-45°]
Skin (reinforcements)	[+45°/-45°/0°/+45°/-45°]
Stringers	[0°/90°]$_{2S}$
Ring:	
Height [mm]	40
Lay-up	[0°/90°]$_{2S}$

Alexey N. Fedorenko, Boris N. Fedulov and Evgeny V. Lomakin

Table 2. Lamina material properties

Parameter	Value
Young's modulus, E_{11} [N/mm^2]	57,765
Young's modulus, E_{22} [N/mm^2]	53,686
Shear modulus, G_{12} [N/mm^2]	3065
Poisson's ratio, ν_{12}	0.048
Density, ρ [kg/m^3]	1510
Ply thickness [mm]	0.33

3.2. Finite element model

Following experimental data described in previous section, a finite element model of cylinder was developed to simulate buckling and postbuckling process using ABAQUS software. Model contains about 18000 S4R-type shell elements with mean size 10mm (Fig.1). Both ends of the cylinder were rigidly fixed to ensure actual gage length of 540mm between reinforcing rings except the vertical degree of freedom for loaded end. Due to convergence problems and low loading rate, a quasy-static implicit solver for dynamic analysis was selected. As initial step of the study, a linear elastic constitutive model is used with properties given in Table 2. Then nonlinear elastic model presented in Section 2 is implemented via UMAT subroutine.

Figure 1. Finite element model of stiffened cylinder

4. Results and discussion

Fig.2 shows the experimental loading diagram for compression, a diagram obtained using linear elastic model, and a diagram obtained using constitutive relations, proposed in Section 2 of this paper. Coefficients presented in Table 3 for proposed model are used. Shear behavior is modelled with $\alpha = 10^{-8}$(MPa^{-3}), realizing diagram shown in Fig.3. The values from Table 3 are not uniquely obtained due to the lack of experimental data for their matching. But these values are in compatibility with available unidirectional data of Table 2 and give a good agreement with experimental results for compression shown in Fig.2. One can suppose the reasons of the divergence of linear model prediction with the use of properties presented in Table 2 and experimental diagram. The first suggestion is that the moduli were obtained on the base of standard tests with the use of specimens of higher thickness, than the shell in analyzed structure. Another possible reason is that only tension moduli presented in Table 2 is used but it can be inappropriate for shell areas that are in compression or combined stress state.

According to experimental observation, it was no any shell damage detected until sudden collapse due to stringer buckling, so for this particular problem damage is neglected.

Alexey N. Fedorenko, Boris N. Fedulov and Evgeny V. Lomakin
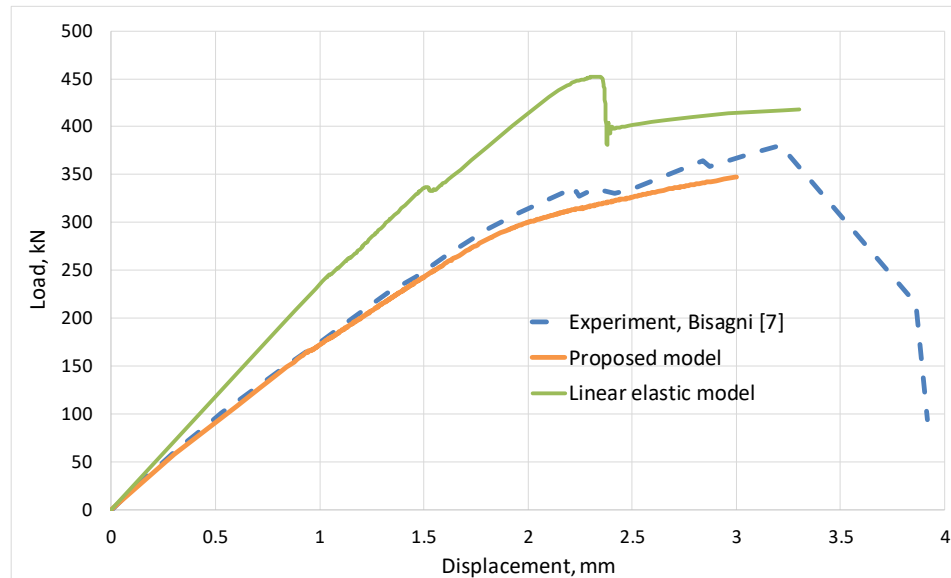
Figure 2. Compressive load versus displacement diagrams

Table 3. Values of coefficients for constitutive relations Eq.6, (1/MPa)

a_{11}^0	a_{22}^0	c_{11}	c_{22}	a_{12}^0	c_{12}^0
3.85E-03	3.85E-03	-4.4E-03	-4.4E-03	-2E-3	2E-3
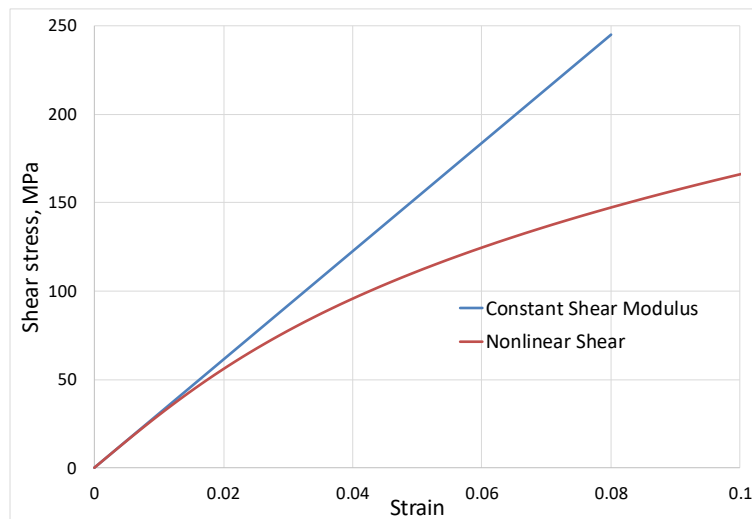
Figure 3. Nonlinear shear diagram from Eq.7 with $\alpha = 10^{-8}$ (MPa-3)

Deflections of the cylindrical shell in normal direction to the surface due to buckling is shown in Fig.4 for the experimental load cell displacement close to failure (3mm). One can see that two elastic models have different buckling shapes. The results obtained with the use of proposed nonlinear anisotropic elastic model of material susceptible to stress state has exactly the same form of buckling deflections as observed in experimental studies [12].

Alexey N. Fedorenko, Boris N. Fedulov and Evgeny V. Lomakin
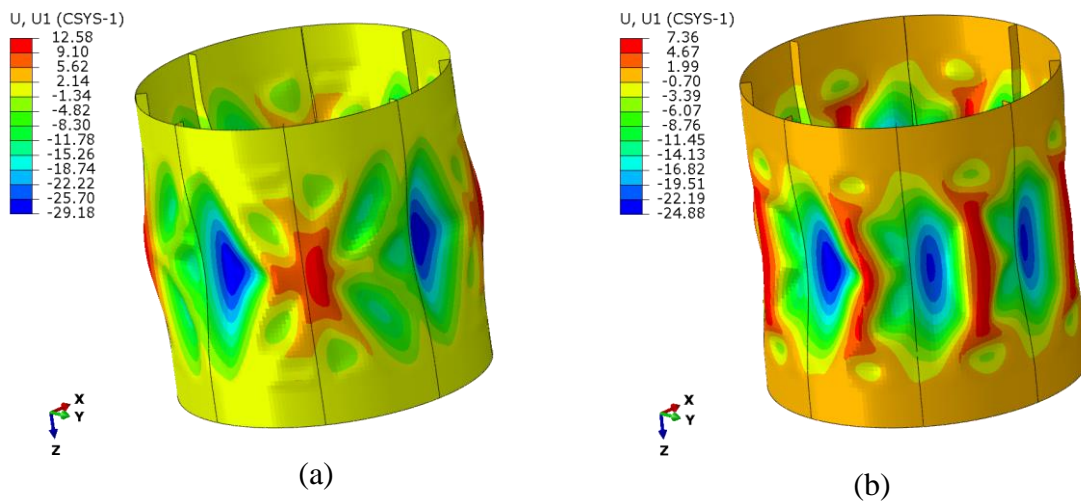
Figure 4. Shell displacements in radial direction due to buckling (scaled to factor 2):
a) Linear model, b) Proposed model

Fig.5 presents triaxiality parameter distribution in outer surface of shell before the final collapse with the use of proposed model. Major areas of shell surface lie close to limiting values, corresponding to biaxial compression $\xi = -2/3$ and biaxial tension $\xi = +2/3$. It means that the usage of experimental data for biaxial loading is very important for accurate simulation.
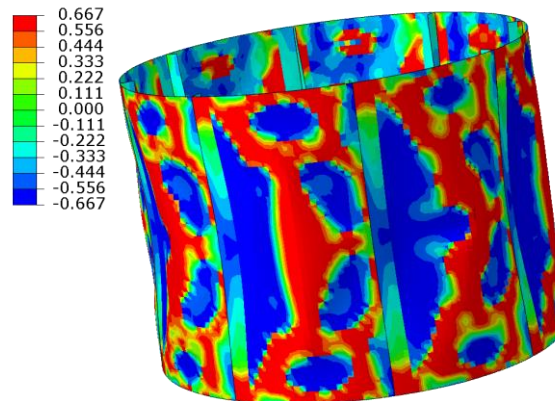
Figure 5. Triaxiality parameter ξ distribution before predicted collapse

Conclusion

The implementation of anisotropic elastic material model susceptible to the stress state and nonlinear shear within FEM software shows a good correlation of theoretical prediction with experimental results in tests of buckling of composite shells. Both loading diagrams and buckling shapes are close to the recorded ones during the composite shell compression test. Development and implementation of proposed model, including damage consideration, looks as effective tool for engineering applications.

Acknowledgments

Alexey N. Fedorenko, Boris N. Fedulov and Evgeny V. Lomakin

References

[1]   R. Degenhardt, R. Rolfes, R. Zimmermann, and K. Rohwer. COCOMAT - Improved material exploitation of composite airframe structures by accurate simulation of postbuckling and collapse. *Composite Structures*, 73(2):175–178, 2006.

[2]   S. S. Wang, S. Srinivasan, H. T. Hu, and R. HajAli. Effect of material nonlinearity on buckling and postbuckling of fiber composite laminated plates and cylindrical shells. *Composite Structures*, 33(1):7–15, 1995.

[3]   R. M. Jones. Stress-Strain Relations for Materials with Different Moduli in Tension and Compression. *AIAA Journal*, 15(1):16–23, 1977.

[4]   H. T. Hahn and S. W. Tsai. Nonlinear Elastic Behavior of Unidirectional Composite Laminae. *Journal of Composite Materials*, 7(1):102–118, 1973.

[5]   W. Vanpaepegem, I. Debaere, and J. Degrieck. Modelling the nonlinear shear stress–strain response of glass fibre-reinforced composites. Part II: Model development and finite element simulations. *Composites Science and Technology*, 66: 1465–1478, 2006.

[6]   B. N. Fedulov, A. N. Fedorenko, M. M. Kantor, and E. V. Lomakin. Failure analysis of laminated composites based on degradation parameters. *Meccanica*, 53:359–372, 2017.

[7]   B. N. Fedulov, A. N. Fedorenko, A. A. Safonov, and E. V. Lomakin. Nonlinear shear behavior and failure of composite materials under plane stress conditions. *Acta Mechanica*, 228(6):2033–2040, 2017.

[8]   B. N. Fedulov, A. A. Safonov, M. M. Kantor, and S. V. Lomov. Modelling of thermoplastic polymer failure in fiber reinforced composites. *Composite Structures*, 163:293–301, 2017.

[9]   E.V. Lomakin, B.N. Fedulov, A.M. Melnikov. Constitutive models for anisotropic materials susceptible to loading Conditions. *In: Belyaev A., Irschik H., Krommer M. (eds). Mechanics and Model-Based Control of Advanced Engineering Systems*. 209-216, 2014.

[10]   E.V. Lomakin, B.N. Fedulov. Plane strain extension of a strip made of a material with stress state type dependent properties and weakened by cuts with circular base. *Mechanics of Solids*, 48(4): 424–430, 2013.

[11]   E. V. Lomakin and B. N. Fedulov. Nonlinear anisotropic elasticity for laminate composites. *Meccanica*, 50(6):1527–1535, 2015.

[12]   C. Bisagni and P. Cordisco. Post-buckling and collapse experiments of stiffened composite cylindrical shells subjected to axial loading and torque. *Composite Structures*, 73(2):138–149, 2006.